Structure and Dynamics of a Detergent-Solubilized Membrane Protein: Measurement of Amide Hydrogen Exchange Rates in M13 Coat Protein by ^{1}H NMR Spectroscopy†

Joe D. J. O'Neil and Brian D. Sykes*

MRC Group in Protein Structure and Function, Department of Biochemistry, The University of Alberta, Edmonton, Alberta T6G 2H7, Canada

Received July 17, 1987; Revised Manuscript Received December 1, 1987

ABSTRACT: The coat protein of bacteriophage M13 is inserted into the inner membrane of *Escherichia coli* where it exists as an integral membrane protein during the reproductive cycle of the phage. The protein sequence consists of a highly hydrophobic 19-residue central segment flanked by an acidic 20-residue N-terminus and a basic 11-residue C-terminus. We have measured backbone amide hydrogen exchange of the protein solubilized in perdeuteriated sodium dodecyl sulfate using ^{1}H nuclear magnetic resonance (NMR) spectroscopy. Direct proton exchange-out measurements in D_2O at 24 °C were used to follow the exchange of the slowest amides in the protein. Multiple exponential fitting of the exchange data showed that these amides (29 ± 3 at pH 4.5) exchanged in two kinetic sets with exchange rates [$(1.2 \pm 0.4) \times 10^{-4}$ s^{-1} and $(4.1 \pm 1.2) \times 10^{-7}$ s^{-1}] that differed by more than 100-fold, the slower kinetic set being retarded 10^5-fold relative to poly(DL-alanine). The exchange rate constant for the slowest set of amides exhibited an unusual pD dependence, being proportional to $[OD^-]^{1/2}$. It is shown that this is an artifact of the multiple exponential fitting of the data, and a new method of presentation of exchange data as a function of pD is introduced. Steady-state saturation-transfer techniques were also used to measure exchange. These methods showed that 15–20 amides in the protein are very stable at 55 °C and that about 30 amides have exchange rates retarded by at least 10^5-fold at 24 °C. Saturation-transfer studies also showed that the pH dependence of exchange in the hydrophilic termini was unusual. This is explained as being due to long-range electrostatic effects arising both from the protein itself and also from the anionic detergent molecules. Hydrogen exchange studies on the products of proteinase K digestion of the protein localized the slowly exchanging amides to the hydrophobic core of the protein. Relaxation [Henry, G. D., Weiner, J. H., & Sykes, B. D. (1986) *Biochemistry 25*, 590–598] and solid-state NMR experiments [Leo, G. C., Colnago, L. A., Valentine, K. G., & Opella, S. J. (1987) *Biochemistry 26*, 854–862] have previously shown that the majority of the protein backbone is rigid on the picosecond to microsecond time scale, except for the extreme ends of the molecule which are mobile. The hydrogen exchange results, which are sensitive to a much longer time scale (>10^{-4} s), suggest a stable core with a progressive increase in amplitude or frequency of motions as the ends of the protein are approached.

The bacteriophage M13 (fd, f1) is a circular single-stranded DNA molecule encapsulated in a regular array of 2700 copies of a major coat protein (gene 8 protein) (Marvin & Wachtel, 1975). During the reproductive cycle of the phage, the coat protein is inserted into the inner membrane of *Escherichia coli* (Webster & Cashman, 1978). The amino acid sequence of the protein (Asbeck et al., 1969; Nakashima & Konigsberg, 1974) includes a highly hydrophobic 19-residue segment similar to the membrane-spanning α-helices identified by X-ray diffraction in the proteins of the photosynthetic reaction center of *Rhodopseudomonas viridis* (Deisenhofer et al., 1985) and similar to the putative membrane-spanning helices identified in the sequences of numerous intrinsic membrane proteins [for a review, see Engelman et al. (1986)]. The hydrophobic core of the molecule endows it with a strong tendency to self-associate; in the absence of dispersive agents, the protein is highly aggregated in water (Cavalieri et al., 1978). Solubilization can be achieved in sodium dodecyl sulfate (SDS)[1] or DOC micelles and in phospholipid vesicles or bilayers. There is some evidence that the protein is a tightly associated dimer in detergent micelles (Makino et al., 1975). Flanking the hydrophobic core of the protein are a 20-residue acidic N-terminal segment and an 11-residue basic C-terminus (Asbeck et al., 1969; Nakashima & Koningsberg, 1974). The positive charges at the C-terminus may be necessary for electrostatic binding to acidic lipid head groups during membrane insertion (Kuhn et al., 1986).

The structural and dynamic properties of the coat protein have been previously examined in its various environments. In the intact phage, solid-state ^{15}N NMR analysis indicates an extended, slewed α-helix from residues 5 to 50, with a bend in the helix at about residue 30 (Colnago et al., 1987; Valentine, 1986). Residues 1–4 are mobile on the 10-kHz time scale and are considered disordered. Laser Raman spectroscopy (Thomas et al., 1983) and X-ray fiber diffraction

† Supported by the Medical Research Council of Canada (MRC Group in Protein Structure and Function) and the Alberta Heritage Foundation for Medical Research (J.D.J.O. is the recipient of an AHFMR postdoctoral fellowship).

[1] Abbreviations: BPTI, basic pancreatic trypsin inhibitor; BUSI IIA, protease inhibitor IIA from bull seminal plasma; CD, circular dichroism; DMPC, dimyristoylphosphatidylcholine; DOC, deoxycholate; DSS, disodium 2,2-dimethyl-2-silapentane-5-sulfonate; HPLC, high-performance liquid chromatography; NMR, nuclear magnetic resonance; PC, phosphatidylcholine; PDLL, poly(DL-lysine); ppm, parts per million; PDLA, poly(DL-alanine); SDS-d_{25}, perdeuteriated sodium dodecyl sulfate.

0006-2960/88/0427-2753$01.50/0

(Marvin et al., 1974) also suggest that the protein is predominantly α-helical as the coat. In DMPC multilamellar bilayers, solid-state ^2H NMR and ^{15}N NMR (Leo et al., 1987) gave a similar structure except that six additional C-terminal residues are mobile. In detergent micelles (both SDS and DOC), the backbone of the protein was found to be rigid on a 100-MHz time scale by ^{13}C NMR spectroscopy; only about four amino acids at each end are able to undergo large-amplitude fluctuations (Henry et al., 1986). CD spectroscopy showed that the protein has a similar structure in DOC micelles and PC vesicles (Nozaki et al., 1976). The CD studies also suggested that as much as 30% of the protein could be in the β-sheet configuration while in the dispersed state although this conclusion has been disputed by other authors using CD data (Williams & Dunker, 1977).

The hydrogen exchange behavior of proteins depends upon structural fluctuations, the time scale of which ranges over many orders of magnitude. The precise nature of these fluctuations is under intense investigation [for reviews, see Englander and Kallenbach (1984), Barksdale and Rosenberg (1982), and Woodward and Hilton (1979)]. Because of its ability to resolve individual protons in proteins, high-resolution NMR spectroscopy is a powerful tool for providing a quantifiable measure of dynamics throughout the entire backbone of a protein. In particular, individual amide exchange measurements have provided insight into the stability, dynamic fluctuations, sensitivity to cofactor binding, or the kinetics of folding of the following proteins and peptides: BPTI (Roder et al., 1985a; Roder & Wüthrich, 1986), BUSI IIA (Wüthrich et al., 1984), apamin (Dempsey, 1986), *lac* repressor head piece (Boelens et al., 1985), myoglobin (Vasant Kumar & Kallenbach, 1985), cytochrome *c* (Wand & Englander, 1986), T4 lysozyme (Griffey et al., 1985), and ribonuclease S (Kuwajima & Baldwin, 1983). Henry et al. (1987b) have measured some relatively rapidly exchanging individual backbone amides in M13 coat protein using a ^{13}C NMR equilibrium isotope shift technique. This technique measures exchange rates by determining the pH at which the [^{13}C]carbonyl resonances adjacent to deuteriated and protonated amides coalesce in a 50:50 mixture of H_2O/D_2O (Feeney et al., 1974; Hawkes et al., 1978). A limitation is that the ^{13}C resonances adjacent to very slowly exchanging amides coalesce at pHs greater than 12 so that it was not possible to measure the exchange rates of the slowest amides. In this paper, we have measured the slowest exchanging amides in the coat protein by exchange-out kinetic measurements in D_2O; some of the faster amides were also measured indirectly by a steady-state ^1H NMR saturation-transfer technique. The results provide a dynamic model of the protein in which the hydrophobic core is very stable whereas the structure of the hydrophilic portions is less stable by several orders of magnitude.

Experimental Procedures

Materials

DSS and perdeuteriated sodium dodecyl sulfate were purchased from MSD Isotopes (Pointe Claire, Dorval, PQ), and perdeuteriated acetic acid was from Stohler Isotope Chemicals (Rutherford, NJ). Bio-Gel P-300 and D_2O were purchased from Bio-Rad Laboratories (Richmond, CA), and Sephadex G-25 was from Pharmacia (Montreal, PQ). Proteinase K (protease type XI) was purchased from Sigma. A synthetic peptide, corresponding to the first 21 amino acids of the coat protein (Asbeck et al., 1969; Nakashima & Konigsberg, 1974), was provided by the Alberta Peptide Institute. Its purity was checked by amino acid analysis, ^1H NMR spectroscopy, and HPLC.

Methods

Protein Purification. Bacteriophage M13 was prepared as described by Henry et al. (1986) except that *E. coli* were grown on rich medium (Miller, 1972). For each NMR sample, about 25 mg of purified phage was dissolved in 1 mL of 100 mM SDS-d_{25} and 10 mM phosphate buffer, pH 7. M13 coat protein was separated from phage DNA by passing the solubilized phage over a column of Bio-Gel P300 (8 × 2.5 cm) equilibrated with 10 mM SDS-d_{25} and 10 mM phosphate, pH 7. Finally, the column eluate containing coat protein was pooled and freeze-dried.

Direct Kinetic Measurements of Hydrogen Exchange. In early experiments, proton efflux from the peptide amides of coat protein was initiated by dissolving the freeze-dried protein sample (see above) in about 0.7 mL of water and passing this over a small (5 mL) Sephadex G-25 column equilibrated in D_2O, 10 mM SDS-d_{25} and the appropriate buffer. This method was used in order to avoid possible artifacts caused by dissolution from the dry state (Englander et al., 1972). However, since we were mainly interested in the slowly exchanging peptide amides and since we did not observe any large differences either in the appearance of the NMR spectrum or in the kinetics of exchange, we subsequently resorted to measuring exchange by dissolving the freeze-dried protein directly in about 0.65 mL of a buffered D_2O solution. We have sometimes observed variability in the exchange kinetics which seemed to be due to protein concentration. Consequently, all hydrogen exchange results reported herein are for protein between 1.2 and 1.5 mM except for the experiment at pD 4.5 which contained 2.1 mM protein. Exchange solutions also contained 20–30 mM phosphate and 10–100 mM acetic-d_4 acid at lower pDs and 50 mM borate at higher pDs. It may be noted that catalysis of hydrogen exchange by buffer ions is negligible due to their low pK_a's relative to the pK_a for the peptide bond amide (Englander & Kallenbach, 1984). Similarly, the effect of ionic strength on the exchange rates of backbone peptides made up of uncharged amino acids is negligible; however, ionic strength may significantly affect exchange rates at peptides comprised of charged amino acids (Kim & Baldwin, 1982). We have measured the effect of SDS on the hydrogen exchange rates of structureless, hydrophobic tripeptides in order to separate the effects of detergent on exchange from the effects of protein structure (O'Neil & Sykes, 1988).

^1H NMR spectra at 400 MHz of freshly dissolved coat protein in 5-mm NMR tubes were recorded with the use of a Varian XL 400 NMR spectrometer. The pulse width was 12 μs (60°), and the acquisition time was 1 s. Usually 200–400 scans (3.3–6.7 min) were required to achieve a reasonable signal to noise ratio in the amide region of the spectrum. During the first hour of exchange, 3–4 spectra were recorded; after this, the number of scans was increased to 1000–2000 (16–33 min), and spectra were recorded periodically for up to several months.

Measurements of pH in D_2O (pD) are uncorrected for both the glass electrode reading error in D_2O and the D_2O isotope effect on the ionization states of molecules (Bundi & Wüthrich, 1979). Chemical shifts were measured relative to the methyl resonance of DSS. Protein concentration was determined by absorbance using A_{280} = 8200 L·mol^{-1}·cm^{-1}.

Steady-State Measurements of Hydrogen Exchange. Hydrogen exchange rates can also be determined by measuring the transfer of saturation by exchange from the H_2O resonance

(Forsen & Hoffman, 1963, 1964; Gadian, 1982). For these measurements, spectra were acquired in 90% H_2O/10% D_2O with preirradiation of the water for 1.3 s. When exchange is on the order of or faster than the spin–lattice relaxation rate of the amide proton, $(T_1^{NH})^{-1}$, the fractional amide intensity (M_Z/M_Z^0) will be reduced to $(1 + k_{ex}T_1^{NH})^{-1}$ due to saturation transfer. An average T_1^{NH} value of about 0.7 s was measured for the amides in 90% H_2O/10% D_2O, pD 6.9 and 30 °C, by standard inversion–recovery methods at 500 MHz on a Varian VXR-500 NMR spectrometer.

NMR spectra were also measured in 90% H_2O/10% D_2O solutions without saturation of the H_2O resonance using a jump and return pulse sequence (Plateau & Gueron, 1982). As this pulse sequence does not excite all of the protons in the spectrum equally, this might introduce inaccuracies in the integration of spectra. However, integration of spectra acquired with excitation optimized at different points in the spectrum showed that these inaccuracies are small; this is because the spectral window of interest (6.6–9.2 ppm) is relatively narrow.

Proteolytic Digestion with Proteinase K. Proteinase K digestion was carried out by using approximately 1:100 enzyme/protein (w/w) at pH 8.9, 37 °C. Proteinase K digests the hydrophilic N- and C-termini of M13 coat protein in SDS-d_{25} micelles, leaving the hydrophobic core intact (Henry et al., 1986, 1987a). Separation of the peptide fragments from the hydrophobic core on a Sephadex G-25 gel filtration column followed by amino acid analysis confirmed this digestion pattern; however, the NMR spectrum of the freeze-dried protein core suggested that extensive aggregation had occurred. Consequently, hydrogen exchange of the hydrophobic core was measured on a mixture of the core and the digested fragments. This was done by digesting the protein with proteinase K in water, 10 mM SDS-d_{25}, and 5 mM phosphate, pH 8.9, for 9 h. Hydrogen exchange was started by passing the mixture over a Sephadex G-25 column equilibrated with D_2O, 10 mM SDS-d_{25}, and 50 mM acetic-d_4 acid. The void volume peak was collected, and ^1H NMR spectra were recorded.

Data Analysis. The ^1H NMR spectrum of fully exchanged coat protein includes 28 nonexchangeable aromatic resonances between 6.8 and 7.6 ppm arising from 1 Trp, 2 Tyr, and 3 Phe residues. Except at the pH_{min}, most of the amides which exchange with half-lives of 10 min or longer appear in the spectrum between 7.5 and 9.2 ppm. The number of amides was calculated by comparing the integrated intensity in the amide region to that for the aromatic region with the assumption that the spin–lattice relaxation times are the same for both types of protons. In fact, the T_1's (measured at 500 MHz) for both types of protons span a small range of values, but most of the amide T_1's are close to 0.7 s and most of the aromatic T_1's were between 0.9 and 1.1 s. The difference in relaxation rate between the two groups would cause an overestimation of the number of amides in a spectrum by not more than 10% for the spectral acquisition conditions used. The absence of exchangeable amides in the aromatic region was checked by comparing, at different times during exchange, the integrated area in the aromatic region to that of a region of the spectrum (3.2–1.85 ppm) where no exchangeable protons are expected. Sometimes, for spectra collected early in the course of an exchange experiment at the pH_{min}, some exchangeable amides occurred in the aromatic region. Therefore, the number of protons between 3.2 and 1.85 ppm had to be calculated first by comparison with the number of hydrogens in the aromatic region at a point in the exchange experiment when the area in the aromatic region was unchanging. Then, using the known number of protons between 3.2 and 1.85 ppm, we could calculate the number of hydrogens in the aromatic region when exchangeable hydrogens were present.

Results

Backbone amide hydrogen exchange measurements are a quantifiable measure of protein structural fluctuations when protein exchange rates are retarded compared to those of unstructured model compounds under identical conditions. Fortunately, exchange rates of non-hydrogen-bonded amides can be accurately predicted taking into account the effects of pH, temperature, and local amino acid sequence including inductive and charge effects [for a review, see Englander and Kallenbach (1984)]. The most commonly used model compound is the random-coil poly(DL-alanine) (Englander & Poulsen, 1969), but poly(DL-lysine) (Kim & Baldwin, 1982), small peptides (Molday et al., 1972), and thermally unfolded BPTI (Roder et al., 1985b) have all provided models of freely exchanging amides which are in close agreement with each other. In this paper, we derive a measure of the stability of secondary structural elements of M13 coat protein by comparing our measured hydrogen exchange rates to those predicted for PDLA using equations from Roder et al. (1985b) and Englander et al. (1979) (see the legend to Figure 3). Elsewhere, we have shown that dodecyl sulfate increases the pH_{min} for exchange by 1.3–1.7 units for an unstructured peptide in an SDS micelle (O'Neil & Sykes, 1988). When base catalysis predominates, a 1 pH unit increase in the pH_{min} translates into a 10-fold "retardation" of exchange due to the detergent. Therefore, in studies of the protein in SDS, a portion of the retardation of exchange rates relative to those calculated for PDLA will be due to the effect of the detergent.

We have used three different NMR experiments to measure amide hydrogen exchange. Each experiment can detect amide protons exchanging slower than certain limiting exchange rates, the limits being quite different for each of the three experiments. Direct exchange-out experiments in D_2O have the lowest upper limit and are unable to measure amides with lifetimes less than about 5 min ($k_{ex} > 2 \times 10^{-3}$ s^{-1}) since this much time is needed to record the first point. This limit is shown as a dotted line in Figure 3. When this limit is compared to the PDLA exchange curves (Figure 3), it becomes clear that, except at the pH_{min} the exchange-out technique can only detect amides whose exchange is retarded by the structure of the protein. The "jump-and-return" experiment, which does not require saturation of the water resonance, has the highest upper limit of the three experiments (see dot–dashed line in Figure 3). This limit depends upon the chemical shift difference between the amide and water resonances (Δ), and the observed amides will be those in slow exchange with the water ($k_{ex} \ll \pi\Delta/2 \cong 1200$ s^{-1}) (Harris, 1983). When spectra are obtained with saturation of the H_2O resonance, the upper rate limit for amide detection lies between the limiting rates for the other two experiments (see dot–dashed line in Figure 3). Whenever $k_{ex} \geq 10(T_1^{NH})^{-1}$, the amide resonance will not be detectable, and rates cannot be measured. Amide exchange will be measurable in the presence of H_2O saturation for any $k_{ex} \leq (T_1^{NH})^{-1}$. However, for amides retarded by more than 10^5-fold compared to those in PDLA, k_{ex} will not equal $(T_1^{NH})^{-1}$ until the pH is greater than 11. Consequently, this experiment also has a lower limit below which it is not practical to measure exchange rates.

^1H NMR Kinetic Measurements of Hydrogen Exchange. Figure 1A shows the aromatic and amide regions of a ^1H NMR spectrum acquired 7 min after dissolution of the coat protein in D_2O at pD 4.8, 24 °C. Most of the exchangeable

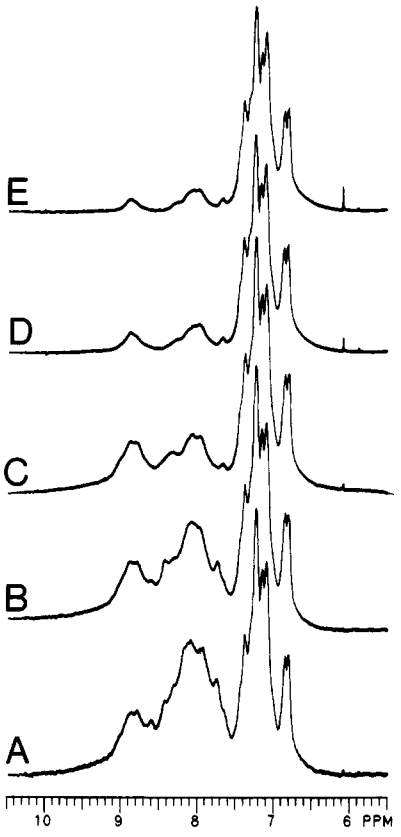

FIGURE 1: Low-field region of 400-MHz ^{1}H NMR spectra of M13 coat protein in SDS-d_{25} micelles showing the time course of amide proton exchange at (A) 7 min, (B) 1.2 h, (C) 21 h, (D) 341 h, and (E) 671 h after dissolution in D_2O at pD 4.76 and 24 °C. The number of scans was 200, 400, 1000, 2000, and 2000 for spectra A, B, C, D, and E, respectively. Protein concentrations was 1.5 mM in SDS-d_{25}, 10 mM acetic-d_4 acid, and 30 mM phosphate. A line broadening of 0.5 Hz was used in processing the spectra.

amide protons appear as two partially resolved groups at 7.5–8.5 ppm and at 8.5–9.2 ppm; a small number of amides apparently overlap the aromatic protons between 6.7 and 7.6 ppm. The region of the spectrum from 7.5 to 8.5 ppm contains about 75% of the total amides observed (spectrum A). During the first 20 h of exchange at pD 4.8 (spectra A–C), the shape of the amide envlope changes because the high-field peak (7.5–8.5 ppm) contains a larger portion of rapidly exchanging amides than does the low-field peak (8.5–9.2 ppm). Consequently, by 20 h of exchange (C), the high-field peak contains only about 60% of the total amides. Later in the exchange experiment (spectra C–E), the shape of the amide envelope remains constant as the intensity of the amides gradually diminishes.

At higher pDs, fewer amides are observed initially (Figure 2A), and the shape of the amide envelope resembles that seen later in the exchange at low pDs (Figure 1D). This suggests that the amides which exchange rapidly at low pD are too fast to measure at higher pDs and the same amides, which are observed to exchange very slowly at low pDs, exchange much faster at higher pDs. Figure 2D shows an exchange difference spectrum in which a spectrum acquired after 133 min of exchange was subtracted from a spectrum acquired initially (8 min). The difference spectrum obtained shows that even early in an exchange experiment at high pD no exchangeable amides are observed in the aromatic region of the spectrum.

The exchange experiments were quantified by integration of the entire amide regions of spectra at increasing times of exchange and then fitting the results to $\sum_i A_i \exp(-k_{ex_i} t)$ (i = 1–3) with a nonlinear least-squares fitting routine. The time

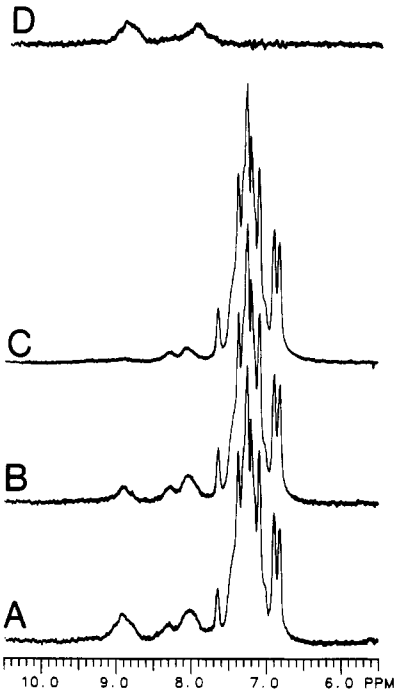

FIGURE 2: Low-field region of 400-MHz ^{1}H NMR spectra of M13 coat protein in SDS-d_{25} micelles showing the time course of amide proton exchange at (A) 8 min (B) 29 min, and (C) 25 h after dissolution in D_2O at pD 8.9 and 24 °C. The number of scans was 200, 200, and 1000, respectively. Protein concentration was 1.2 mM in SDS-d_{25} and 50 mM borate. The spectra were processed with a line broadening of 0.5 Hz. Spectrum D is a spectrum produced by subtracting a spectrum acquired at 2.3 h (not shown) from spectrum A.

for each point was chosen as the midpoint of the acquisition period. Each set of exchange data was fit with 1-, 2-, and 3-exponential decays and the best fit chosen by using the standard deviations of the fits. The results of amide exchange measurements over the range of pDs from 3.7 to 9.2, at 24 °C, are summarized in Table I and Figure 3. At low pDs, about 35 of the protein's 50 amide protons exchange slowly enough to be measured. Table I and Figure 3 show that most of the measurable amides segregate into two sets with exchange rates that differ by at least 10-fold. As the pD of the exchange reaction is elevated, the total number of amides with measurable exchange rates decreases. At pD 9.2, only one set of exchanging amides can be observed. Figure 3 also contrasts the pD dependence of exchange in poly(DL-alanine) (Englander et al., 1979; Roder et al., 1985b) with that of the coat protein. Besides the marked retardation of exchange in the protein compared to the unstructured polypeptide, the dependence upon deuterium oxide concentration is different: the slowest kinetic set in the protein shows an apparent $[OD^-]^{1/2}$ dependence whereas the polypeptide shows $[OD^-]$ dependence.

Exchange experiments were also done at higher temperatures. Figure 4A shows a spectrum of the protein obtained 5 min after dissolution in D_2O at pD 3.7 and 24 °C. Figure 4B,C shows spectra of the same sample at different times after the temperature had been elevated to 55 °C. Insofar as the amides in these spectra resolve into two groups from 7.5 to 8.5 ppm and from 8.5 to 9.2 ppm, they resemble the spectra acquired at room temperature at high pD (Figure 2) and those acquired late in exchange at low pD (Figure 1). However, because of the narrower line widths achieved at higher temperatures, the two groups are completely separated, and individual resonances begin to resolve within the groups. Kinetic analysis of this experiment was difficult since the protein was observed to precipitate after several days at high temperature.

Table I: Multiple Exponential Least-Squares Fits of Proton Exchange Data as a Function of pH[a]

pD	k_{ex_1} (s^{-1})	n_1	k_{ex_2} (s^{-1})	n_2	$\sum_i n_i$
3.55	$(3.3 \pm 1.1) \times 10^{-4}$	15 ± 2	$(3.7 \pm 0.8) \times 10^{-6}$	21 ± 1	36 ± 3
4.41	$(4.7 \pm 2.1) \times 10^{-4}$	14 ± 3	$(1.0 \pm 0.3) \times 10^{-6}$	16 ± 1	30 ± 4
4.51	$(1.2 \pm 0.4) \times 10^{-4}$	16 ± 2	$(4.1 \pm 1.2) \times 10^{-7}$	13 ± 1	29 ± 3
4.76	$(2.0 \pm 1.4) \times 10^{-4}$	13 ± 4	$(5.1 \pm 2.0) \times 10^{-6}$	20 ± 3	33 ± 7
6.42	$(1.1 \pm 0.2) \times 10^{-4}$	13 ± 1	$(3.1 \pm 0.8) \times 10^{-6}$	7 ± 1	20 ± 2
6.74	$(3.7 \pm 1.9) \times 10^{-4}$	10 ± 2	$(9.8 \pm 4.2) \times 10^{-6}$	8 ± 2	18 ± 4
7.50	$(3.4 \pm 1.0) \times 10^{-4}$	6 ± 1	$(2.4 \pm 0.4) \times 10^{-5}$	6 ± 1	12 ± 2
7.84	$(2.8 \pm 0.7) \times 10^{-4}$	9 ± 1	$(6.5 \pm 1.7) \times 10^{-6}$	7 ± 0.5	16 ± 1.5
8.85	$(1.2 \pm 0.7) \times 10^{-3}$	5 ± 2	$(6.4 \pm 2.1) \times 10^{-5}$	3 ± 1	8 ± 3
9.22			$(1.7 \pm 0.6) \times 10^{-4}$	4 ± 1	4 ± 1
2.83[b]			$(1.3 \pm 0.5) \times 10^{-5}$	18 ± 2	18 ± 2
3.70[c]	$(3.2 \pm 2.6) \times 10^{-4}$	6 ± 2	$(8.1 \pm 2.4) \times 10^{-6}$	16 ± 2	22 ± 4

[a] k_{ex_i} (i = 1, 2) values are the first-order rate constants; n_i values are the number of amides exchanging at a particular rate. The errors were determined from the standard deviations of the fits. [b] Hydrogen exchange was measured on a proteinase K digest of the protein in SDS-d_{25}. [c] Data obtained at 55 °C; all other data were obtained at 24 °C.

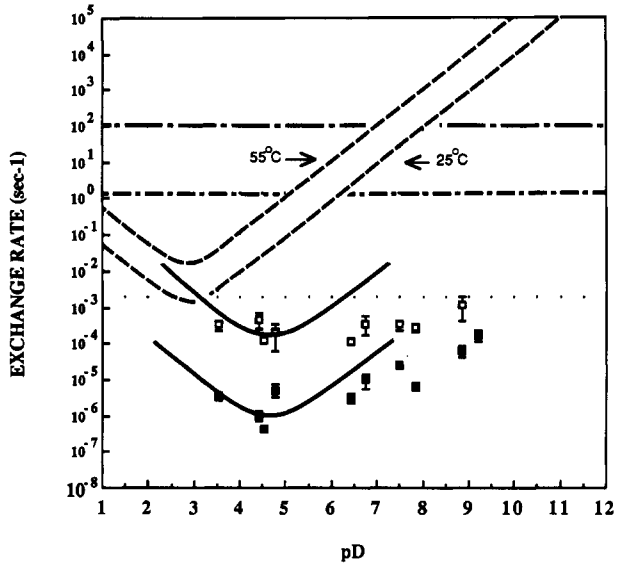

FIGURE 3: Plot of log k_{ex_i} vs pD from the data in Table I with the open squares representing the rapidly exchanging set (k_{ex_1}) and the closed squares the slowly exchanging set (k_{ex_2}). The error bars were calculated from the standard deviations of the fits in Table I [see Snedecor and Cochran (1979)]. The solid lines through the two sets of data are PDLA exchange curves adjusted for the shift in the pH_{min} of the data as well as for retardation of exchange. The deviations of the data from the PDLA curves are an artifact arising from the fitting of the data to multiple exponentials as explained in the text and demonstrated in Figure 7. For comparison, theoretical curves (---) for the exchange of poly(DL-alanine) are shown at 25 and 55 °C. The equations for these curves are $k_{ex}^{25} = (6.419 \times 10^8)10^{pD-14.873} + (0.588)10^{-pD}$ and $k_{ex}^{55} = (9.673 \times 10^8)10^{pD-13.968} + (5.966)10^{-pD}$ for exchange at 25 and 55 °C, respectively. These equations are calculated from Roder et al. (1985b), and the temperature dependence of the D_2O dissociation constant, k_{D_2O}, was calculated according to Covington et al. (1966). The horizontal lines indicate the upper limits of amide exchange detectability for the three experiments used to measure exchange: (···) exchange-out technique; (–·–) saturation-transfer technique; (—·—) jump and return experiment (exchange broadening).

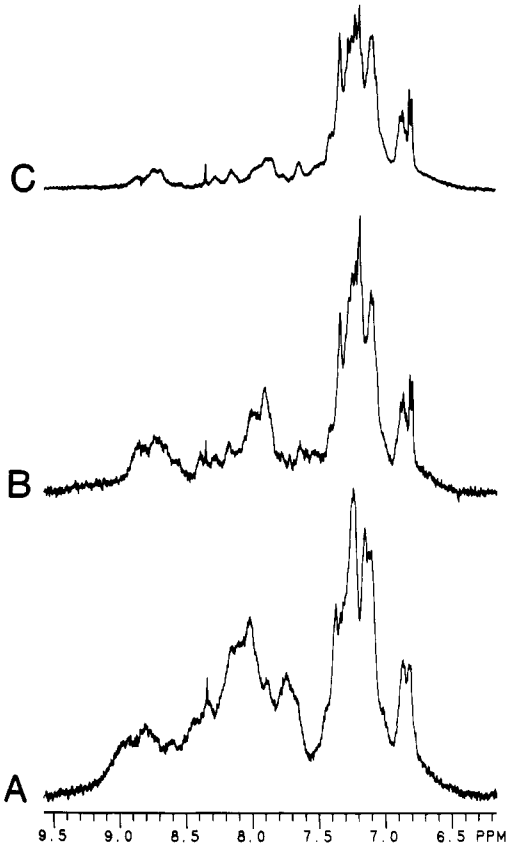

FIGURE 4: Low-field region of 400-MHz ^1H NMR spectra of M13 coat protein in SDS-d_{25} micelles showing the time and temperature dependence of amide proton exchange. (A) 6 min after dissolution in D_2O at 24 °C; (B) 14 min after dissolution and just after the solution had equilibrated to 55 °C; and (C) 17.1 h after dissolution at 55 °C. The number of scans was 200, 200, and 2000, respectively. Protein concentration was 1.4 mM in SDS-d_{25}, 117 mM acetic-d_4 acid, and 64 mM phosphate, pD 3.7. The line broadening was 0.5 Hz.

However, analysis of the first 18 h of exchange (see Table I) and examination of spectrum C of Figure 4 strongly suggest that the protein contains a set of 10–15 very stable amides which exchange about 10000 times slower than in an unstructured polypeptide at this temperature.

Steady-State Measurement of Hydrogen Exchange. A set of about 15 stable amides was also observed in H_2O solutions when the relatively rapidly exchanging amides were eliminated from the spectrum by using steady-state techniques in contrast to the previous kinetic isolations in D_2O. Figure 5A shows a spectrum of the protein obtained in 90% H_2O/10% D_2O at 55 °C, pH 7.5, using a "jump-and-return" pulse sequence. This sequence does not require saturation of the water which would be transferred to any amides which are in fast exchange (relative to $1/T_1^{NH}$) with the water. The distribution of amides (and the appearance of the spectrum) is similar to that observed in early exchange experiments acquired at low pDs (see Figure 1A). A difficulty in the integration of this spectrum is the overlap between the "aromatic region" (6.8–7.6 ppm) and the "amide region" (7.6–9.2 ppm) of the spectrum. This difficulty was overcome by assuming first that all Tyr, Ser, Thr, Lys, Asp, and Glu side chain exchangeable protons as well as the exchangeable protons at the termini of the molecule are exchange broadened under the conditions of the experiment (Wüthrich & Wagner, 1979). The exchangeable indole proton

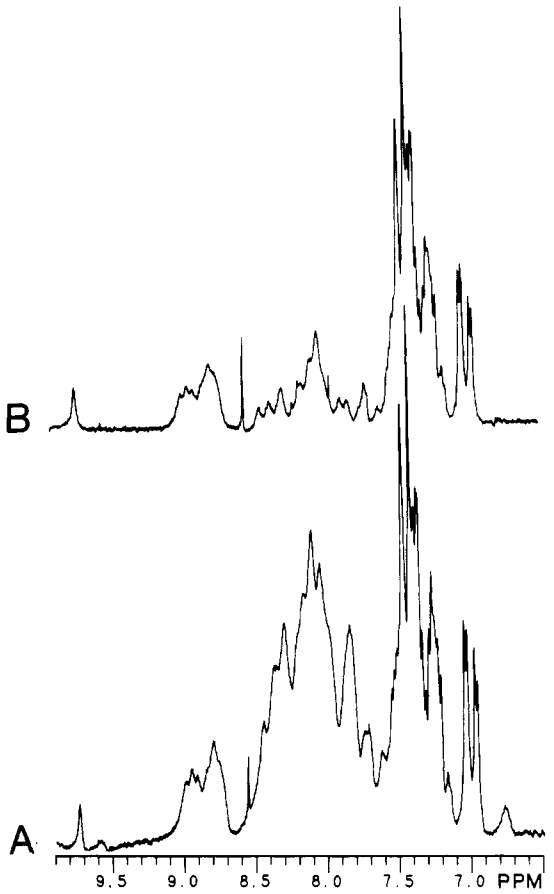

FIGURE 5: Aromatic and amide regions of the 400-MHz ^{1}H NMR spectrum of the coat protein in SDS-d_{25} micelles in 90% H_2O/10% D_2O. Spectrum A was acquired without solvent irradiation using a jump and return pulse sequence. Protein concentration was 2.7 mM in SDS-d_{25}, with 141 mM phosphate, pH 7.5 at 55 °C. Spectrum B was acquired by using presaturation of the solvent resonance. All other conditions were as in (A). The narrow resonance observed in the spectra at about 8.53 ppm is due to formate in the sample. The spectra were processed with a 1-Hz line broadening and were baseline-corrected by using a first-order polynomial fitting procedure.

of Trp-26 has been identified at 9.75 ppm (Cross & Opella, 1981), and one of the two Gln protons is probably at 6.68 ppm based on random-coil chemical shift measurements in peptides (Bundi & Wüthrich, 1979). If next we assume that the aromatic region consists of the 28 nonexchangeable aromatic protons plus one proton from the Gln side chain, we can estimate that the minimum number of peptide amides is 36 from 7.5 to 8.6 ppm and 5 from 8.6 to 9.1 ppm. Under these conditions, up to nine protons might be exchanging too rapidly to be observed. Indeed, any protons which are not hydrogen bonded under the conditions of this experiment are probably eliminated by exchange broadening (see Figure 3), and all of the amides which are observed must be retarded at least 10-fold compared to PDLA.

By use of the same sample as in Figure 5A, the more rapidly exchanging protons were eliminated by preirradiation of the water resonance, and spectrum B was obtained. Compared to spectrum A, about 29 amides have disappeared from the spectrum because their exchange rates are ≥ 7 s^{-1}. Present in the spectrum is a set of about 13 more stable amides whose exchange rates are ≤ 1.4 s^{-1}. In fact, because of the improved resolution at 55 °C, up to 20 amide protons, perhaps at varying degrees of exchange, can be counted in spectrum B. Interestingly, the low-field peak loses the equivalent of 1 amide in intensity, the other 28 being lost from the high-field peak. This preponderance of slowly exchanging amides in the downfield peak (also observed in the exchange-out experiments) is a reflection of the fact that hydrogen bonding of amide protons causes downfield shifts in their resonances (Wagner et al., 1983) and suggests that hydrogen bonding is an important factor in the retardation of exchange in the coat protein. This experiment shows that at pH 7.5, 55 °C, the protein consists of a core of stable amides whose hydrogen exchange rates are retarded by at least 500-fold whereas the rest of the structure is less stable, the exchange rates being retarded by less than 500-fold. The approximately 29 amides which are lost to presaturation but which are present in the "jump-and-return" experiment must be retarded by 10–500-fold compared to the amides in PDLA. This suggests that the core of the protein is very stable whereas the hydrophilic termini are more loosely structured.

The spectrum shown in Figure 6A was acquired under conditions similar to those for Figure 5B except that the temperature was 24 °C and the pH was 7.1. Lowering the temperature moved a number of amides from fast to slow exchange compared to $(T_1^{NH})^{-1}$. In addition to the large number of broader amide resonances present in Figure 6A, one very narrow doublet resonance is present at 8.05 ppm. This resonance disappears at lower pHs, suggesting that it has an unusually high pH_{min}. The narrow line width of this peak and the high pH_{min} point to this resonance belonging to an amide in the unstructured N-terminus of the protein (see Discussion). Spectrum A also appears to contain several other narrow resonances protruding from the broad amide envelope at 24 °C. Other narrow resonances appear in the spectrum when the pH is lowered (see inset at 8.7 ppm) so that altogether two very narrow and about five narrow resonances have been observed. These narrow resonances probably arise from the four amino acids at each end of the molecule which are known to be disordered.

The number of amides exchanging faster than $(T_1^{NH})^{-1}$ can be altered by changing the pH and thereby changing k_{ex}. In Figure 6B, the dashed curves show the calculated pH dependence of amide resonance intensity in a saturation-transfer experiment for a 50-residue PDLA at 25 and 55 °C. The midpoints of the transitions catalyzed by OH^- and H^+ at 25 °C are pH 6.2 and pH −0.2, respectively; between these two transitions is a plateau of 2.5 pH units where amide exchange is too slow to be affected by saturation of the water resonance. The pH dependence of amide intensity in the protein at 24 °C is strikingly different from that of the random-coil polypeptide (Figure 6). The range of pHs over which full amide intensity is observed is very narrow in the protein and is shifted to higher pH. Also, the alkaline limb of the protein titration curve appears to consist of multiple transitions. For example, the plateau in the data between pH 8 and pH 10.5 suggests that the protein contains at least 2 sets of amides whose exchange rates differ by more than 1000-fold; about 22 amides have been saturated at pH 8 whereas the remaining 28 amides do not begin to be saturated until pH 10.5 is reached. The end of the plateau at pH 10.5 is about 5 pH units higher than that calculated for PDLA, and this suggests that about 30 amides in the protein are retarded by 10^5-fold compared to the amides in PDLA at pH 10.5.

Hydrogen Exchange of the Proteolyzed Protein. The amide regions of ^{1}H NMR spectra of the proteinase K digested protein in D_2O appeared very similar to the spectra of the intact protein shown in Figure 1C–E. Proton exchange-out data obtained from the proteinase K digested protein at pD 2.83 fit to a single-exponential decay with $k_{ex} = (1.3 \pm 0.5) \times 10^{-5}$ s^{-1} for 18 ± 2 amides (see Table I). Exchange mea-

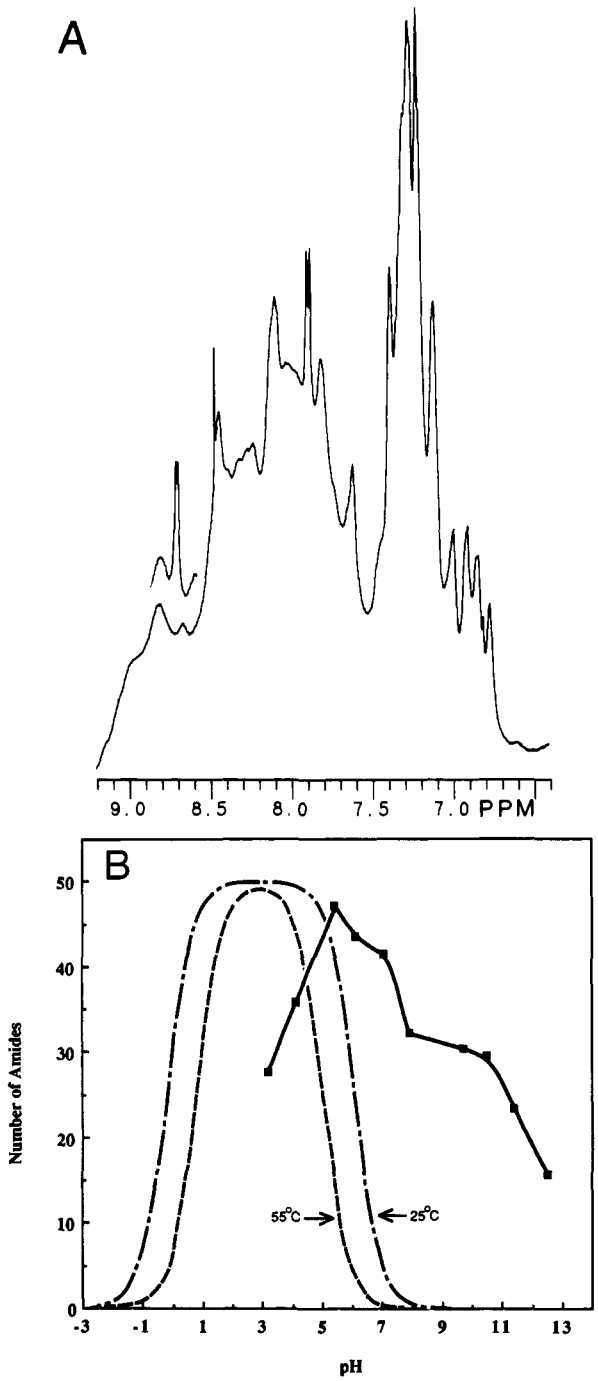

FIGURE 6: (A) Aromatic and amide regions of the 400-MHz ^{1}H NMR spectrum of the M13 coat protein in SDS-d_{25} micelles acquired in 90% H_2O/10% D_2O with presaturation of the water resonance. Protein was in 157 mM phosphate at 24 °C at pH 7.12. The inset shows the portion of a spectrum at pH 3.2. The asterisk indicates a sharp resonance from the formate ion. (B) Plot of the pH dependence of amide proton resonance intensity for M13 coat protein. Spectra were acquired in 90% H_2O/10% D_2O at 24 °C with presaturation of the solvent. Protein concentration was 2.1 mM in SDS-d_{25} with 121 mM phosphate. The dashed lines show the predicted loss in amide intensity for hypothetical 50-residue random-coil poly(DL-alanines) at 25 (–·–) and 55 °C (- - -) calculated as described under Methods, taking the k_{ex}^{25} and k_{ex}^{55} values as a function of pH from Figure 3 and assuming T_1^{NH} = 1 s.

sured on a synthetic peptide corresponding to residues 1–21 by direct exchange-out methods and by saturation-transfer measurements was approximately at the PDLA limit. This confirms that the measured exchange on digested protein originated from the intact core of the molecule and not from the released peptides.

Discussion

To obtain information about the structure and dynamics of M13 coat protein, we have measured backbone amide hydrogen exchange using ^{1}H NMR spectroscopy at 24 and 55 °C. At 55 °C, individual amide resonances could be observed in the NMR spectra. However, protein aggregation at high temperatures restricted the measurement of exchange to shorter periods of time than was possible at lower temperatures. This problem was overcome by using steady-state experiments to measure hydrogen exchange at 55 °C. At room temperature, individual amide resonances were not observed in either one- or two-dimensional ^{1}H NMR spectra at 400 MHz. We therefore analyzed the hydrogen exchange data obtained at room temperature by integrating the entire amide regions of ^{1}H NMR spectra over the time course of an exchange experiment and then fitting the results to multiple exponential decays.

The fitting of hydrogen exchange data from large macromolecules to a linear combination of exponential decays has been discussed by Laiken and Printz (1970). They simulated hydrogen exchange decay curves by using a random distribution of rate constants and then showed that the curves could be well fit with only two or three distinct kinetic classes. Most of the published exchange profiles for large proteins can also be fit with two- or three-exponential decays, but, unfortunately, the kinetic classes thus obtained have no clear physical meaning. Multiple exponential analysis of hydrogen exchange data from small molecules is much more likely to be physically meaningful. However, even for small molecules, a kinetic class analysis will be justified only if independent evidence can be obtained that the molecule has a small number of discrete kinetic classes.

In the M13 coat protein, several lines of evidence suggest that there are two distinct kinetic classes of exchanging amides. The spectra in Figure 5 show that the saturation-transfer and exchange broadening limits can be used to arbitrarily separate the amides in the coat protein into classes with different exchange rate limits. Integration of spectrum A shows that up to 9 backbone amides are exchange broadened at 55 °C; about 41 amides must be retarded by more than 10-fold over PDLA. Integration of spectrum B suggests that about 37 amides are exchanging faster than the T_1^{NH} limit (less than 500-fold retardation over PDLA) and up to 20 amides are exchanging slower than this limit. That there is not a continuous distribution of amides with exchange rates scattered about the T_1^{NH} limit is suggested by the kinetic analysis of exchange at 55 °C which shows that about 16 ± 2 amides are retarded by nearly 10 000-fold over PDLA. Therefore, at 55 °C, a large portion of the protein is very unstable, exchange rates being retarded by less than 500-fold compared to PDLA. A smaller portion of the protein is very stable; at 55 °C, about 20 amides are retarded by 10^4-fold over PDLA.

Visual inspection of the spectra in Figure 1 also suggests that two distinct kinetic classes of amides exist in the protein. Early in the exchange experiment the changing shape of the amide region suggests that a rapid set of amides is being flushed out, leaving behind a distinct slow set. However, among the 20 or so slow amides, no individual resonances are ever resolved in the spectra. This suggests that the individual amide resonances are quite broad at 24 °C and that their protons exchange over a narrow range of rates. Otherwise, if 10 or fewer amides exchanged more than 100-fold more slowly than the rest of the group, individual amides would be resolved in the spectra. The effective molecular weight of the protein (≃28 000; Makino et al., 1975) and the rotational

correlation time (11 ns; Henry et al., 1986) are large owing to the association of SDS, and this explains the broadened line widths in the spectra.

The amino acid sequence of the coat protein suggests that large differences in stability could exist in different segments of the protein. The forces which stabilize the structure in the hydrophilic termini of the molecule are probably predominantly H bonds with perhaps some electrostatic contributions, whereas in the hydrophobic central segment the H bonds are likely to be reinforced by numerous hydrophobic contacts. On this basis, it seems likely that the structure in the hydrophobic segment is more stable than that in the termini and that the two kinetic classes of amides arise from the hydrophobic and hydrophilic segments. Generally, hydrophobic interactions are strengthened by temperature increases whereas hydrogen bonds are weakened at higher temperatures (Kauzmann, 1959). It is therefore possible that the difference in the stability of these two segments of the protein is greater at 55 °C than at 24 °C and further evidence is necessary before a kinetic class analysis of the exchange experiments at 24 °C can be accepted.

The pH dependence of saturation transfer at 24 °C (Figure 6B) also suggests that the hydrophobic domain is considerably more stable than the rest of the protein. The plateau in the data in Figure 6B between pH 8 and pH 10.5 shows that about 28 amides are 1000 times more stable than the amides in the rest of the protein. In this experiment, the stable domain appears to have increased in length by about 10 residues compared to its length measured by saturation transfer at 55 °C and measured at 24 °C by the exchange-out method. This might be because the multiple exponential fit underestimates the true length of this segment (for reasons discussed below), and perhaps the stable domain is indeed shorter at higher temperatures.

The exchange experiments on proteinase K digests of the protein show that the most stable amides are not distributed throughout the sequence of the protein but rather reside in the hydrophobic core. This experiment also demonstrates that exchange from the core of the protein is entirely independent of the exchange in the C-terminal segment since its removal appeared to have no effect on exchange from the core. Finally, Henry et al. (1987b) have measured some individual amide exchange rates in the coat protein and have shown that among the first 20 amino acids and the last 5 residues, no exchange rate is retarded by more than 500-fold compared to PDLA. On the other hand, for a segment of 15 residues in the core of the molecule, exchange is not less than 10000-fold retarded. Taken together, all of these results suggest that there are two kinetic classes of amides in the protein.

The multiple exponential fits of the exchange-out data presented in Figure 3 are of double exponentials at each pD except the highest one. At low pDs (3.55–4.76), the rate constants of the two kinetic classes differ by 50–500-fold (Table I). The slow class represents the hydrophobic core of the molecule while the fast class contains the slowest members of the hydrophilic termini of the protein and are probably immediately adjacent to the hydrophobic core. About 15–20 amides exchange too rapidly to be observed using the exchange-out technique even at the exchange pD_{min}. Among the unobserved amides are about four amino acids on both termini of the molecule which, according to much of the structural and dynamic data on the protein (see the introduction), are disordered in solution and are therefore exchanging at the PDLA limit. This interpretation of the exchange data suggests that the most stable part of the molecule is the central hydrophobic core and that the flexibility of the protein increases progressively as the ends are approached.

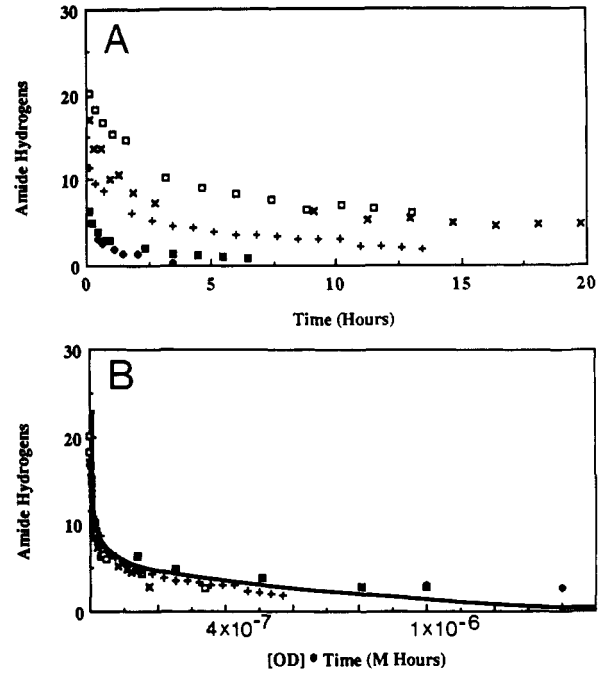

FIGURE 7: Time course for hydrogen exchange of M13 coat protein in SDS-d_{25} micelles as a function of pD. (A) Amide proton intensity versus time; (B) amide proton intensity versus the product of the deuterium oxide concentration and time. The experiments were done at pD 6.42 (□), 6.74 (×), 7.5 (+), 8.9 (■), and 9.2 (◊) (see Table I). The line through the data in panel B is a two-exponential least-squares fit with $n_1 = 12 \pm 1$, $n_2 = 6.1 \pm 0.7$, $k_{ex_1} = (2.8 \pm 0.2) \times 10^4$ M^{-1} s^{-1}, and $k_{ex_2} = (1.4 \pm 0.5) \times 10^2$ M^{-1} s^{-1}.

Although the standard deviations of the fits are small at low pD (Table I, Figure 3), the deviations are largest late in the exchange experiment. Triple-exponential fits of the data at low pD fit the data over the entire exchange-out period, but the standard deviations of the fits are much larger than for the double-exponential fits partly because fewer points were recorded late in the experiments. The effect of the third exponential is to "split" the slowest set into two sets as well as to reduce the size of the fastest set. All of these observations are diagnostic of variability in exchange rates in the two main kinetic classes deduced above. This is especially noticeable at higher pDs where only the 20 slowest amides can be measured. We find that this slow set fits much better to two exponentials than to one. However, the difference in exchange rates between these two sets is only 14–40-fold, suggesting that the slowest kinetic set encompases amides exchanging over a 50-fold range of rates.

Table I shows that the total number of amides in each kinetic class decreases as the pD is elevated from 6.42 to 9.22. If two kinetic classes exist over this pD range, then we would have to postulate a pD-dependent conformational change to explain the changing class sizes. In addition, a similar argument would be necessary to explain the unusual pD dependence of the classes which show $[OD^-]^{1/2}$ dependence rather than the usual $[OD^-]$ dependence. It can be shown that both of these effects are an artifact of the multiple exponential fitting of the data. Figure 7A shows part of the time courses for exchange corresponding to five of the experiments in Table I at high pD. If the data follow the normal pD dependence of PDLA, then the effect of a unitary pD increase is to shift the measurement of a given value of NH(t) to one-tenth the time at which it occurred at the lower pD. Thus, two exchange curves measured at pDs that differ by 1 unit can be made to

superimpose by multiplying the times for the data collected at the higher pD by a factor of 10. Generally, sets of exchange curves at different pDs can be tested for true $[OD^-]^n$ dependence by plotting NH(t) vs $[OD^-]^n t$ where t is time. In Figure 7B, we have plotted NH(t) vs $[OD^-]t$ for the data in Figure 7A; within the experimental scatter of the data, these curves superimpose. The data do not fall on the same curve if NH(t) vs $[OD^-]^{1/2}t$ is plotted, and this shows that the apparent pD dependence of the data in Figure 3 is an artifact of the fitting procedure. This arises from the fact that more amides exchange faster than the detection limit as the pD is raised; naturally, the fit of the distribution of remaining amides shows fewer amides with a weighted average rate slower than before. However, despite these problems with the multiple exponential fits, the direct exchange-out data clearly show that the pD_{min} for exchange in the protein is significantly higher than that for PDLA.

Of course, it is possible that the tendency of the stable amides in the protein to separate into two kinetic classes might reflect the true nature of exchange in the putative α-helical membrane-spanning portion of the protein. Two classes of amides have been observed in single α-helices in the *lac* repressor head piece (Boelens et al., 1985) and in BPTI (Wagner et al., 1984): Residues on the hydrophobic faces of helices were observed to exchange slower than residues on the hydrophilic faces. In the coat protein, the two classes of slowly exchanging amides might represent amides at the protein interface of a dimer and those exposed to the SDS molecules.

The pH dependence of exchange in M13 coat protein is unusual for several reasons. The protein sequesters all of the acidic amino acids in the N-terminus (1–20) and most of the basic residues in the C-terminus (40–50), leaving the highly hydrophobic core (21–39) of the molecule entirely uncharged. The effects of long-range electrostatic interactions on k_{ex} in PDLL were studied by Kim and Baldwin (1982). They showed that the pH_{min} for k_{ex} in PDLL is 2 pH units lower than the pH_{min} for uncharged PDLA in the absence of salt. Apparently, this is because the pH near the surface of the PDLL molecule is higher than the measured pH of the bulk solution due to the condensation of hydroxyl ions by the positively charged PDLL molecule. Considering the sequence of the coat protein, we can expect the pH_{min} for exchange of the amino acids in the core to be similar to that for PDLA (pH_{min} 3) whereas the pH_{min} in the acidic and basic domains should be perturbed to higher and lower pHs, respectively. To these effects must be added the effect of SDS. In studies on structureless hydrophobic peptides in SDS (O'Neil & Sykes, 1988), we observed a peptide amide hydrogen exchange pH_{min} of about 4.5 in 100 mM salt solutions. In agreement with this result, we observe a pH_{min} for the hydrophobic core (slowest set of amides) in Figure 3 at about pH 4.5–5.0. SDS would be expected to alter exchange in the basic C-terminus by pushing the pH_{min} back up toward pH 3 whereas the pH_{min} for the acidic N-terminus should be at or above pH 4.5. These predictions are also confirmed in the steady-state measurement of exchange shown in Figure 6. The very small region of full amide intensity compared to the PDLA curve can be explained if there are two domains of rapidly exchanging amides in the protein; an acidic domain with an unusually high pH_{min} would account for the loss in amide intensity between pH 5 and 3, and a small basic domain with a relatively unperturbed pH_{min} would account for the loss in intensity between pH 5 and 7.

Conclusions

The hydrogen exchange properties of M13 coat protein in SDS micelles suggest a model of the protein in which the central hydrophobic domain is several orders of magnitude more stable than the hydrophilic domains and in which the flexibility of the protein increases progressively as the ends of the protein are approached. This model is in good agreement with the hydrogen exchange results of Henry et al. (1987b). The solid-state ^2H and ^{15}N NMR studies of the protein in DMPC bilayers (Leo et al., 1987) and the solution ^{13}C NMR studies of the protein in detergent micelles (Henry et al., 1986) all suggest that the protein backbone is uniformly rigid except at the very ends of the molecule. The difference probably arises from the time scales over which hydrogen exchange, relaxation, and solid-state NMR are sensitive to motion in the backbone. Since large-amplitude fluctuations on the picosecond to microsecond time scale are eliminated by the relaxation and solid-state NMR techniques, hydrogen exchange must occur either by large-amplitude low-frequency motions ($<10^4$ Hz) or by very small-amplitude higher frequency motions. The latter motions are precisely those which are proposed to account for exchange in the penetration models of hydrogen exchange (Woodward & Hilton, 1979; Karplus & McCammon, 1981; Matthew & Richards, 1983). However, the results of Henry et al. (1987b) suggest that exchange in the C-terminus of the protein is enabled by fraying at the end of a helix, which does not seem likely to occur by small-amplitude high-frequency motions. This leaves the large-amplitude low-frequency motions to account for hydrogen exchange in the coat protein, and these would seem to be better described by the local unfolding models for hydrogen exchange (Englander & Kallenbach, 1987; Roder et al., 1985a).

Acknowledgments

We thank Gerry McQuaid for upkeep of the XL400 spectrometer, Dr. Joel Weiner for providing facilities for growing *E. coli*, and Dr. Robert Hodges for providing the synthetic peptide used in this study. We are grateful to Dr. Gillian Henry for many helpful discussions, to Dr. S. J. Opella for providing numerous preprints prior to publication, and to Sue Smith for typing the manuscript.

Registry No. SDS, 151-21-3.

References

Asbeck, F., Beyreuther, K., Kohler, H., von Wettstein, G., & Braunitzer, G. (1969) *Hoppe-Seyler's Z. Physiol. Chem. 350*, 1047–1056.

Barksdale, A. D., & Rosenberg, A. (1982) *Methods Biochem. Anal. 28*, 1–113.

Boelens, R., Gros, P., Sheek, R. M., Verpoorte, J. A., & Kaptein, R. (1985) *J. Biomol. Struct. Dyn. 3*, 269–280.

Bundi, A., & Wüthrich, K. (1979) *Biopolymers 18*, 285–297.

Cavalieri, S. J., Goldthwaite, D. A., & Neet, K. E. (1976) *J. Mol. Biol. 102*, 713–722.

Colnago, L. A., Valentine, K. G., & Opella, S. J. (1987) *Biochemistry 26*, 847–854.

Covington, A. K., Robinson, R. A., & Bates, R. G. (1966) *J. Phys. Chem. 70*, 3820–3824.

Cross, T. A., & Opella, S. J. (1981) *Biochemistry 20*, 290–297.

Deisenhofer, J., Epp, O., Miki, K., Huber, R., & Michel, H. (1985) *Nature (London) 318*, 618–624.

Dempsey, C. E. (1986) *Biochemistry 25*, 3904–3911.

Engelman, D. M., Steitz, T. A., & Goldman, A. (1986) *Annu. Rev. Biophys. Biophys. Chem. 15*, 321–353.

Englander, J. J., Calhoun, D. B., & Englander, S. W. (1979) *Anal. Biochem. 92*, 517–524.

Englander, S. W., & Paulson, A. (1969) *Biopolymers 7*, 329–339.

Englander, S. W., & Kallenbach, N. R. (1984) *Q. Rev. Biophys. 16*, 521–655.
Englander, S. W., Downer, N. W., & Teitelbaum, H. (1972) *Annu. Rev. Biochem. 41*, 810–924.
Feeney, J., Partington, P., & Roberts, G. C. K. (1974) *J. Magn. Reson. 13*, 268–274.
Forsen, S., & Hoffman, R. A. (1963) *J. Chem. Phys. 39*, 2892–2901.
Forsen, S., & Hoffman, R. A. (1964) *J. Chem. Phys. 40*, 1189–1196.
Gadian, D. G. (1982) *NMR and Its Applications to Living Systems*, pp 131–132, Clarendon, Oxford.
Griffey, R. H., Redfield, A. G., Loomis, R. E., & Dalquist, F. W. (1985) *Biochemistry 24*, 817–822.
Harris, R. K. (1983) *Nuclear Magnetic Resonance Spectroscopy*, p 118, Pitman, London.
Hawkes, G. E., Randall, E. W., Hull, W. E., Gattegno, D., & Conti, F. (1978) *Biochemistry 17*, 3986–3992.
Henry, G. D., Weiner, J. H., & Sykes, B. D. (1986) *Biochemistry 25*, 590–598.
Henry, G. D., Weiner, J. H., & Sykes, B. D. (1987a) *Biochemistry 26*, 3619–3626.
Henry, G. D., Weiner, J. H., & Sykes, B. D. (1987b) *Biochemistry 26*, 3626–3634.
Karplus, M., & McCammon, J. A. (1981) *CRC Crit. Rev. Biochem. 9*, 293–349.
Kauzman, W. (1959) *Adv. Protein Chem. 14*, 1–63.
Kim, P. S., & Baldwin, R. L. (1982) *Biochemistry 21*, 1–5.
Kuhn, A., Wickner, W., & Kreil, G. (1986) *Nature (London) 322*, 335–339.
Kuwagima, K., & Baldwin, R. L. (1983) *J. Mol. Biol. 169*, 218–297.
Laiken, S. L., & Printz, M. P. (1970) *Biochemistry 9*, 1547–1553.
Leo, G. C., Colnago, L. A., Valentine, K. G., & Opella, S. J. (1987) *Biochemistry 26*, 854–862.
Makino, S., Woolford, J. L., Tanford, C., & Webster, R. E. (1975) *J. Biol. Chem. 250*, 4327–4332.
Marvin, D. A., & Wachtel, E. J. (1975) *Nature (London) 253*, 19–23.
Marvin, D. A., Pigram, W. J., Wiseman, R. L., Wachtel, E. J., & Marvin, F. J. (1974) *J. Mol. Biol. 88*, 581–600.
Matthew, J. B., & Richards, F. M. (1983) *J. Biol. Chem. 258*, 3039–3044.
Miller, J. H. (1972) *Experiments in Molecular Genetics*, Cold Spring Harbor Laboratory, Cold Spring Harbor, NY.
Molday, R. S., Englander, S. W., & Kallen, R. G. (1972) *Biochemistry 11*, 150–158.
Nakashima, Y., & Konigsberg, W. (1974) *J. Mol. Biol. 88*, 598–600.
Nozaki, Y., Chamberlain, B. K., Webster, R. E., & Tanford, C. (1976) *Nature (London) 259*, 335–337.
O'Neil, J. D. J., & Sykes, B. D. (1988) *Biochemistry* (submitted for publication).
Plateau, P., & Gueron, M. (1982) *J. Am. Chem. Soc. 104*, 7310–7311.
Roder, H., & Wüthrich, K. (1986) *Proteins: Struct., Funct., Genet. 1*, 34–42.
Roder, H., Wagner, G., & Wüthrich, K. (1985a) *Biochemistry 24*, 7396–7407.
Roder, H., Wagner, G., & Wüthrich, K. (1985b) *Biochemistry 24*, 7407–7411.
Snedecor, G. W., & Cochran, W. G. (1979) *Statistical Methods*, 6th ed., p 138, The Iowa State University Press, Ames, IA.
Thomas, G. J., Prescott, B., & Day, L. A. (1983) *J. Mol. Biol. 165*, 321–356.
Valentine, K. G. (1987) Ph.D. Thesis, University of Pennsylvania, Philadelphia, PA.
Vasant Kumar, N., & Kallenbach, N. R. (1985) *Biochemistry 24*, 7658–7662.
Wagner, G., Pardi, A., & Wüthrich, K. (1983) *J. Am. Chem. Soc. 105*, 5948–5949.
Wagner, G., Stassinopoulou, C. I., & Wüthrich, K. (1984) *Eur. J. Biochem. 145*, 431–436.
Wand, A. J., & Englander, S. W. (1986) *Biochemistry 25*, 1100–1106.
Webster, R. E., & Cashman, T. S. (1978) in *The Single Stranded DNA Phage* (Denhardt, D. T., Dressler, D., & Ray, D., Eds.) pp 557–569, Cold Spring Harbor Laboratory, Cold Spring Harbor, NY.
Williams, R. W., & Dunker, A. K. (1977) *J. Biol. Chem. 252*, 6253–6255.
Woodward, C. K., & Hilton, B. D. (1979) *Annu. Rev. Biophys. Bioeng. 8*, 99–127.
Wüthrich, K., & Wagner, G. (1979) *J. Mol. Biol. 130*, 1–18.
Wüthrich, K., Strop, P., Ebina, S., & Williamson, M. P. (1984) *Biochem. Biophys. Res. Commun. 122*, 1174–1178.